THE UNIVERSITY OF READING

School of Mathematics, Meteorology & Physics

A Moving Mesh Method for the Discontinuous Galerkin Finite Element Technique

Alison Brass

August 2007

Funded by the Natural Environment Research Council (NERC)

This dissertation is a joint MSc in the Departments of Mathematics & Meteorology and is submitted in partial fulfilment of the requirements for the degree of Master of Science.

Acknowledgements

I would like to thank my supervisors Pete Sweby and Mike Baines for their many thoughts and ideas, and also, my friends and family for their support and encouragement when everything seemed to be going wrong. Thank you :)

Declaration

I confirm that this is my own work and the use of all material from other sources has been properly and fully acknowledged.

Alison Brass

Abstract

In this dissertation, velocity-based moving mesh methods for the discontinuous galerkin finite element technique are investigated and applied to solving linear and nonlinear conservations laws with periodic boundary conditions. Two main approaches for the method are considered. The first approach is cell-based and uses a conservation principle on each cell to derive the boundary speeds. The second approach is boundary-based, finding boundary speeds dependent on the local discontinuity in the numerical solutit

Contents

List of Figures

Chapter 1

Introduction

Many equations used in atmosphere and ocean modelling, including the Euler equations of gas dynamics and the shallow water equations, are conservation laws derived assuming the conservation of a particular quantity. Increasingly, Finite Element Methods (FEM) are being employed to solve such equations due to their ability to handle complex geometries. Research is ongoing into ways to improve the accuracy of the numerical solution without significantly increasing the computational cost and generally follows one of two routes.

Conservation laws often have discontinuous numerical solutions even if the initial data is smooth and continuous. Using standard FEM which work in the continuous domain, there is a limitation on how well sharp gradients and shocks can be captured, so it would seem natural to model the solution in a discontinuous manner. The Discontinuous Galerkin (DG) method developed by Reed and Hill [15] is an example of such a technique.

The other approach commonly used is to apply grid adaptation techniques to the standard FEM. Such techniques may include mesh refinments or the use of higher order polynomial approximations in the region of the shock, and Arbitrary Lagrangian-Eulerian (ALE) methods [16], also known as moving meshes, which cluster nodes around the feature and follow the feature as it moves over time.

In more recent years, research has looked at combining these two approaches to provide even better results, incorporating grid adaptation techniques into the discontinuous FEM. The use of a moving mesh algorithm with the DG technique was investigated by Li and Tang [14] who looked at mapping-based methods. We shall also consider the use of moving mesh algorithms but choose to focus on velocity-based methods instead.

In this dissertation we firstly look at the stationary DG method and in Chapter 2 we consider the Runge-Kutta Discontinuous Galerkin (RKDG) method developed by Cockburn and Shu [11]. In Chapter 3 we discuss various grid adaptation techniques before progressing to include some velocity-based moving mesh algorithms into the DG method in Chapters 4 and 5.

In Chapter 4, we focus on cell-based methods and derive the boundary velocities through imposing a conservation principle on each cell. We derive a cell-based method, and some variations, using the local Lax Friedrichs numerical flux at cell boundaries. Additionally, we derive a cell-based method where no flux calculations are required. Through solving simple linear and nonlinear test cases, we evaluate the success of these cell-based methods.

In Chapter 5, we derive a moving DG method without the use of the conservation principle seen in Chapter 4. In this method, the velocities may be obtained from an external source, and we consider a boundary-based method where the boundary speeds may be taken as the notional shock speed associated with the discontinuity in the numerical solution. The results of numerical tests are given in Chatper 6 where we also consider the case of zero boundary speeds and compare with the stationary RKDG method from Chapter 2.

Application of the boundary-based moving mesh method to a 1D system of nonlinear equations is considered in Chapter 7, where the method is derived for the shallow water equations. Some results of preliminary tests for the tidal bore problem and dam-break problem are given in Chapter 8.

Finally, in Chapter 9, we make some general conclusions and consider possible future work.

Chapter 2

The Stationary RKDG Method

2.1 History

The Discontinuous Galerkin (DG) method falls within the category of finite element techniques, using local basis functions to approximate the exact solution on each element. Developed by Reed and Hill [15] for solving the linear neutron transport equation $\sigma u + \nabla\cdot(au) = f$ where σ is real and a is linear, the DG method is noteably different from continuous methods in that it allows the numerical solution to be discontinuous across element boundaries.

Having been used for linear problems, the DG method was then extended to solve nonlinear problems including hyperbolic conservation laws which required

smooth function v(x) and integrating over the cell interval:

$$\int_{I_j} \left(\frac{\partial u}{\partial t} + \frac{\partial f(u)}{\partial x} \right) v \, dx = 0.$$

Using integration by parts we obtain

$$\int_{I_j} \frac{\partial u}{\partial t} v \, dx - \int_{I_j} f \frac{\partial v}{\partial x} \, dx + f v \Big|.$$

(hting(g66.311076(h)-3330099(g)-333.512(S)0.fi2898

The numerical flux may be calulated in many ways, with the Lax-Friedrichs and Godunov schemes providing typical forumlae. Although the accuracy of the

$\forall j = 1 \ldots N$,

2.2.2 Time Integration

We may rewrite (2.7, 2.7) as

$$\frac{du_h}{dt} = L_h(u_h) \qquad \text{in } [0, T]$$
$$u_h(0) = u_h \ ,$$

and partition $[0, T]$ into M equal intervals of size Δt.

To step through time and find $u_h(t = T)$, we will use the total variation diminishing (TVD) Runge-Kutta scheme given in [5].

For $m = 0, \ldots, M - 1$ compute u_h^m from u_h^m as fo310.9091TfΩ7.1189(f)00034986]TJΩ/R5510.9091ual

2.3 RKDG Results on a Stationary Mesh

2.3.1 Linear Advection

We consider the RKDG method applied to the simple linear advection problem

$$
\begin{aligned}
u_t + (3u)_x &= 0 \qquad \text{on } [0,1] \times [0, 0.335] \\
u(x,0) &= 3\sin(2\pi x) + 1 \qquad \text{on } [0,1]
\end{aligned}
$$

with periodic boundary conditions.

At $t = 0.335$ s, we would expect the intial data to have completed slightly more than a single revolution as the wave speed = 3, and as the data should be simply advected, we expect no change in the amplitude of the sine wave. Figure 2.3 shows that the stationary RKDG method has been able to acurately capture the wave speed, advecting the intial data with no significant loss of amplitude.

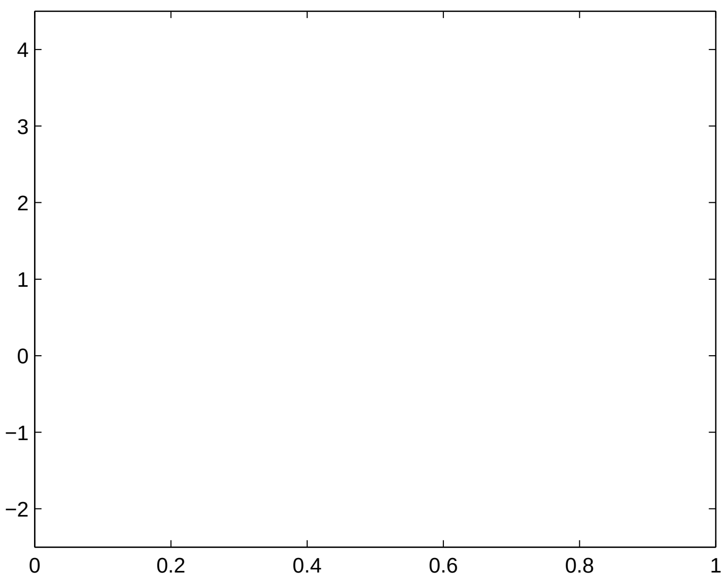

2.3.2 Inviscid Burgers

As a second test case, we consider the stationary RKDG method applied to the nonlinear advection problem and so will eventually move out of the region of densly packed nodes into a region covered by larger cells and the accuracy of the shock capture will decrease. This provides the motivation for our investigations into a moving mesh method which would alow the mesh to move with the shock over time.

2.3.3 Stability

For the linear advection problem where $f(u) = cu$, using linear polynomial approximations and the 2nd order RKDG method, Chavent and Cockburn [4] showed the stability condition to be given by

$$c\frac{\Delta t}{\Delta x} \leq \frac{1}{3}. \tag{2.8}$$

The results of numerical investigations for our linear advection test case showed the method was stable for

under the category of r-refinement, which are also commonly known as moving meshes. In these methods, the number of nodes is kept constant but they are redistbuted so that they are clustered around features of interest. There are two main approaches to moving mesh methods; one is based on mappings, the other on velocities.

3.1 Mapping-based moving mesh techniques

Mapping-based moving mesh methods have three main features. Firstly, there is a 1:1 mapping between nodes in the logical or computational domain, which are equally spaced, to the nodes in the physical domain, where they may be clusted in areas of interest. Li and Tang [14] give this mapping as

$$\xi : x \to \xi, \quad \Omega \to \Omega_c,$$

where Ω denotes the physical domain, Ω_c denotes the logical domain, and where ξ may be found by solving the elliptic system

$$\nabla_x (m \nabla_x \xi) = 0.$$

Here, m is a monitor function, the second key feature of the method, which is used to guide the cell redistiubution. The third feature is interpolation of the numerical

3.2.1 Cell-based techniques

In Chapter 4, we look at some cell-based techniques, where the boundary speeds

Chapter 4

Cell-based Moving Mesh Methods

We now combine a cell-based moving mesh grid adaptation technique with a DG method similar to the RKDG method seen in Chapter 2.

The conservation law problem

$$u_t + f(u)_x = 0 \qquad \text{on } [0,1] \times [0,T] \tag{4.1}$$

$$u(x,0) = u\ (x) \qquad \text{on } [0,1] \tag{4.2}$$

is now solved with periodic boundary conditions on a moving mesh.

For a cell-based moving mesh method, we make use of a conservation principle on each cell and, following the example of Baines et al. [2], seek to move the cell boundaries such that

$$\frac{d}{dt} \int_{x_{j-1/2}}^{x_{j+1/2}} vu \, dx = 0 \tag{4.3}$$

holds for all time.

In the stationary DG method, we derived and solved a weak form of our conservation law problem for u_h. Now, we will instead derive a weak form of the problem in terms of boundary speed $\dot{x}$ which we will solve and then use with the conservation

Due to the conservation principle (4.3) and the fact that $v(x)$ moves with $\frac{dx}{dt}$, this simplifies to give

$$0 = \int_{x_{j-1/2}}^{x_{j+1/2}} v \left(\frac{\partial}{\partial x}(u\dot{x}) + \frac{\partial u}{\partial t} \right) dx. \tag{4.5}$$

Combining (4.5) with (4.4), we obtain

$$-\int_{x_{j-1/2}}^{x_{j+1/2}} v \frac{\partial}{\partial x}(u\dot{x})\, dx = -f v\Big|_{x_{j-1/2}}^{x_{j+1/2}} + \int_{x_{j-1/2}}^{x_{j+1/2}} f \frac{\partial v}{}$$

$$\frac{d}{dt}\int_{x_{j-1/2}}^{x_{j+1/2}} v_h u_h \, dx = 0 \tag{4.10}$$

$$\int_{x_{j-1/2}}^{x_{j+1/2}} u_h(x,0) v_h \, dx = \int_{x_{j-1/2}}^{x_{j+1/2}} u \ (x) v_h \, dx. \tag{4.11}$$

The analytic flux f is not defined at cell boundaries due to the discontinuity in u_h, so we introduce a numerical flux scheme $h(x) = h(u_h(x)^-, u_h(x) \ ) \approx f(u_h(x))$. As for the stationary DG method, we choose to use the local Lax Friedrichs formula given in [5] as

$$h \quad (a, b) = \frac{1}{2}[f(a) + f(b) - c(b - a)]$$

For the simple case when v_h

$$\begin{pmatrix} \Delta_j(t) & 0 \\ 0 & -\Delta_j(t) \end{pmatrix} \begin{pmatrix} w_j(t) \\ w_j(t) \end{pmatrix} = \begin{pmatrix} \Delta_j(t=0) w_j(t=0) \\ -\Delta_j(t=0) w_j'(t=0) \end{pmatrix} \tag{4.13}$$

$$\begin{pmatrix} w_j(0) \\ w_j(0) \end{pmatrix} = \begin{pmatrix} \frac{1}{2}\left(u\left(x_{j+1/2\sqrt{3}}\right) + u\left(x_{j-1/2\sqrt{3}}\right)\right) \\ \frac{\sqrt{3}}{2}\left(u\left(x_{j+1/2\sqrt{3}}\right) - u\left(x_{j-1/2\sqrt{3}}\right)\right) \end{pmatrix}. \tag{4.14}$$

The weak formulation provides cell-by-cell matrix systems for determining the boundary speeds $\dot{x}$, which we may then use to find the updated numerical approximation u_h. We consider two ways of solving for the boundary speeds:

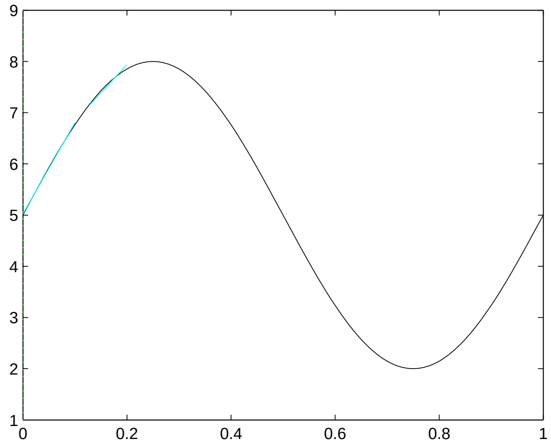
9
8
7
6
5
4
3
2
1
0
0.2
0.4
0.6
0.8
1

We may def[illegible] dim[illegible] space V_h to [illegible]

$$[illegible] 1) : v|_{I_j} \in P^k(I_j),\ j = 1, \ldots [illegible]$$

where P^k is [illegible] polynomials up to degree k, and [illegible] the smooth $v(x)$ [illegible] nction $v_h \in V_h$ and the exact solutio[illegible] erical approximati[illegible]

From the or[illegible] vation law (4.1), we may replace $\frac{\partial u_h}{\partial t}$ a[illegible]

$$[illegible] \int_{x_{j-1/2}}^{x_{j+1/2}} v_h \left(\frac{\partial}{\partial x}(u_h \dot{x}) - \frac{\partial f(u_h)}{\partial x} \right) dx.$$

Alternativel[illegible] e written as

$$[illegible] = \int_{x_{j-1/2}}^{x_{j+1/2}} v_h \left[(u_h \dot{x}) - f(u_h) \right]_x dx. \qquad [illegible] 4.15)$$

One possibl[illegible] equation (4.15) is to take

$$\dot{x} = \frac{f(u_h)}{u_h}.$$

We may use [illegible] twice at each [illegible]

4.2.3 Results

The non-DG method is first applied to a linear advection test problem where we seek to solve

$$u_t + (3u)$$

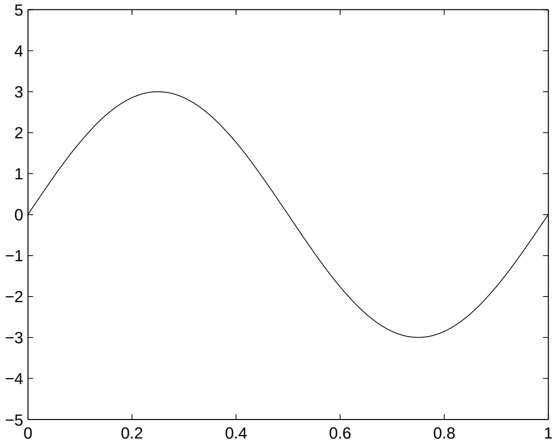
5
4
3
2
1
0
−1
−2
−3
−4
−5
0
0.2
0.4
0.6
0.8
1

Chapter 5

A Boundary-based Moving Mesh Method

In the previous moving mesh methods investigated in Chapter 4, the boundary speeds have been derived based on the conservation principle (4.3) and this has directly linked cell width to the value of the numerical solution on that cell by (4.13). If we wish to overwrite boundary speeds with alternative values e.g. to prevent boundary overtaking, we must therefore derive a new moving mesh algorithm which does not depend on the conservation principle (4.3).

5.1 Derivation of a full-DG Method

The conservation law problem

$$
\begin{aligned}
u_t + f(u)_x &= 0 \qquad \text{on } [0,1] \times [0,T] \\
u(x,0) &= u\ (x) \qquad \text{on } [0,1]
\end{aligned}
$$

is again solved with periodic boundary conditions on a moving mesh.

5.1.1 The inclusion of boundary speeds

To include boundary speeds $\dot{x}$ we use Leibniz rule

$$\frac{d}{dt}\int_{x_{j-1/2}}^{x_{j+1/2}} m\,dx = m\dot{x}|_{x_{j+1/2}} - m\dot{x}|_{x_{j-1/2}} + \int_{x_{j-1/2}}^{x_{j+1/2}} \frac{\partial m}{\partial t}\,dx$$

to expand

$$\frac{d}{dt}\int_{x_{j-1/2}}^{x_{j+1/2}} vu\,dx$$

which is no longer assumed to be zero for all time.

Taking $m = vu$ where $v(x)$ moves with $\frac{dx}{dt}$, we have

$$\begin{aligned}
\frac{d}{dt}\int_{x_{j-1/2}}^{x_{j+1/2}} vu\,dx &= vu\dot{x}|_{x_{j+1/2}} - vu\dot{x}|_{x_{j-1/2}} + \int_{x_{j-1/2}}^{x_{j+1/2}} \frac{\partial}{\partial t}vu\,dx \\
&= \int_{x_{j-1/2}}^{x_{j+1/2}} \frac{\partial}{\partial x}(vu\dot{x})\,dx + \int_{x_{j-1/2}}^{x_{j+1/2}} \frac{\partial}{\partial t}(vu)\,dx \\
&= \int_{x_{j-1/2}}^{x_{j+1/2}} \left(v\frac{\partial}{\partial x}(u\dot{x}) + \frac{\partial v}{\partial x}u\dot{x} + v\frac{\partial u}{\partial t} + \frac{\partial v}{\partial t}u \right) dx \\
&= \int_{x_{j-1/2}}^{x_{j+1/2}} v\left(\frac{\partial}{\partial x}(u\dot{x}) + \frac{\partial u}{\partial t} \right) dx + \int_{x_{j-1/2}}^{x_{j+1/2}} u\left(\frac{\partial v}{\partial t} + \dot{x}\frac{\partial v}{\partial x} \right) dx.
\end{aligned}$$

As $v(x)$ moves with $\frac{dx}{dt}$, the last integral term is zero and substituting in for $\frac{\partial u}{\partial t}$ from our orginal conservation law, we obtain

$$\frac{d}{dt}\int_{x_{j-1/2}}^{x_{j+1/2}} vu\,dx = \int_{x_{j-1/2}}^{x_{j+1/2}} v\,(\dot{x}u - f)_x\,dx.$$

It may be possible to solve this equation by using quadrature to evaluate the integral on the right-hand side directly. However, we choose to follow the ideas of the stationary RKDG derivation and use integration by parts to obtain

$$\frac{d}{dt}\int_{x_{j-1/2}}^{x_{j+1/2}} vu\,dx = -\,v\,(f - \dot{x}u)|_{x_{j-1/2}}^{x_{j+1/2}} + \int_{x_{j-1/2}}^{x_{j+1/2}} (f - \dot{x}u)\,\frac{\partial v}{\partial x}\,dx. \qquad (5.1)$$

We now have a problem for u which includes $\dot{x}$ as required.

5.1.2 The weak formulation

Defining the finite dimensional subspace V_h to be where $\varphi_l(x) = P_l\left(\frac{2(x-x_j)}{\Delta_j}\right)$ and w_j^l are coefficients to be found.

Through the orthgonality properties of the Legendre polynomials we are able to express our problem (5.2, 5.3) as a matrix system

$$\forall j = 1, \dots, N$$

$$\begin{pmatrix} 1 & 0 \\ 0 & l \end{pmatrix} \begin{pmatrix} \dot{\Delta}_j w_j + \Delta_j \dot{w}_j \\ \dot{\Delta}_j w_j + \Delta_j \dot{w}_j \end{pmatrix} = - \begin{pmatrix} h(x_{j+1/2}) - h(x_{j-1/2}) \\ h(x_{j+1/2}) + h(x_{j-1/2}) \end{pmatrix}$$

5.2 Boundary Speed Selection

Unlike previous moving mesh algorithms, this method does not generate the boundary speeds. Instead they may be input from an external source at each timestep, and then the changes to the numerical solution u_h are found accordingly.

In particular, we note that if we take $\dot{x} = 0$ for all boundaries and for all time, the method reverts back to the stationary DG method with Euler timestepping and should yield similar results to the RKDG method from Chapter 2, allowing for the di□erence in accuracy and stability between the Euler and Runge-Kutta time-stepping algorithms.

5.2.1 Selecting non-zero boundary speeds

At each boundary, the numerical solution u_h is discontinous and a jump in the solution occurs (see Figure 2.2). A natural choice for the boundary speed would be the notional shock speed associated with this discontuntiy in u_h. In the case when the jump in u_h is negligible, we can instead use the overall wave speed.

We therefore select the boundary speeds to be

$$\dot{x} = \begin{cases} f'(u_h) & \text{if } u_h - u_h^- \approx 0 \\ \frac{[f(u_h)]}{[u_h]} & \text{otherwise} \end{cases} \tag{5.6}$$

where $[u_h]$ and $[f(u_h)]$ denote the jumps in u_h and $f(u_h)$ respectively.

5.2.2 Controlling cell distribution

Over time, the choice of boundary speeds may result in boundaries overtaking one another or cell widths becoming negligbly small. We need to overcome these issues.

To avoid cells of negligible width, it would may seem natural to remove a boundary

stability. However, if $\Delta t < \Delta t_{\min}$, we use $\Delta t_{\min}$ and must amend the boundary speeds.

Ideally, we only wish to amend the boundary speeds in problematic regions where

Chapter 6

boundaries have remained fixed at their initial locations and it is only through considering the absolute difference between the solutions for u_h at the nodes, as in Figure 6.2, that we are able to see any difference in the numerical approximations found by the RKDG and full DG methods.

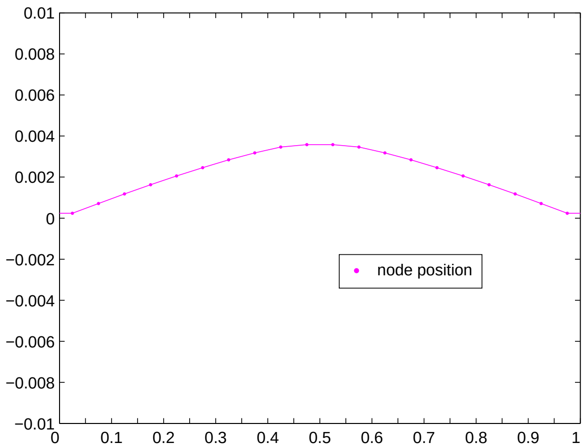

Figure 6.2: The absolute difference in solution between the 2nd order RKDG method and the full-DG method with $\dot{x} = 0$, for the inviscid burgers problem $f(u) = \frac{1}{2}u^2$ at $t = 0.25$ taking $\Delta x = 0.05$ and $\Delta t = 0.0005$.

Numerical investigations into stability indicate that for a linear $f(u) = cu$, the stability of the full-DG method with $\dot{x} = 0$ is comparable with that of the 2nd order RKDG method which is given in [4] as

$$c\frac{\Delta t}{\Delta x} \le \frac{1}{3}$$

is becoming very steep, although the vertical shock has not yet formed.

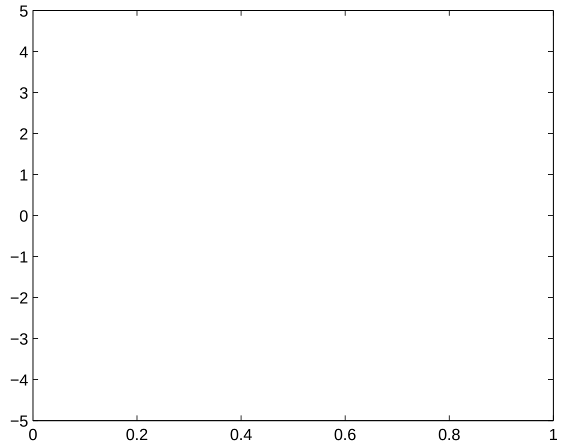

and then at adopting a fixed boundary speed across all boundaries.

6.3.1 Adjustments through speed averaging

We first use the average speed technique to amend boundary speeds around problem cells which would otherwise become too small at the next timestep.

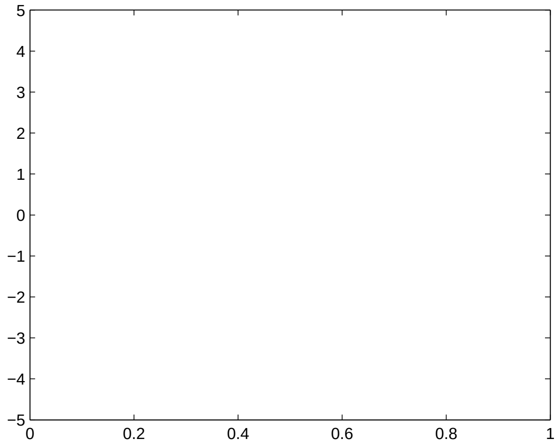

Although the shock capture is generlly not as good as the results seen for the stationary methods, even though the nodes are more densly concentrated, this method has the potential to allow di erent regions of the mesh to move at di erent average speeds, allowing multiple features of interest to be followed which may prove useful in some situations.

6.3.2 Adjustments through adopting a fixed speed

We now consider using the adoption of a fixed speed to control the cell distribution.

Using the fixed speed method, all boundaries are moved with a uniform velocity determined by an approximation to the shock speed. For the test case given by

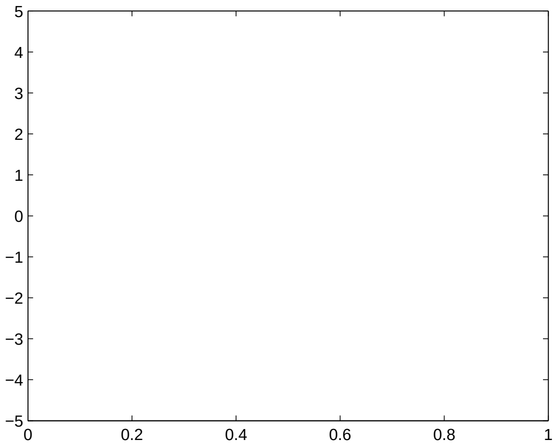
5
4
3
2
1
0
−1
−2
−3
−4
−5
0
0.2
0.4
0.6
0.8
1

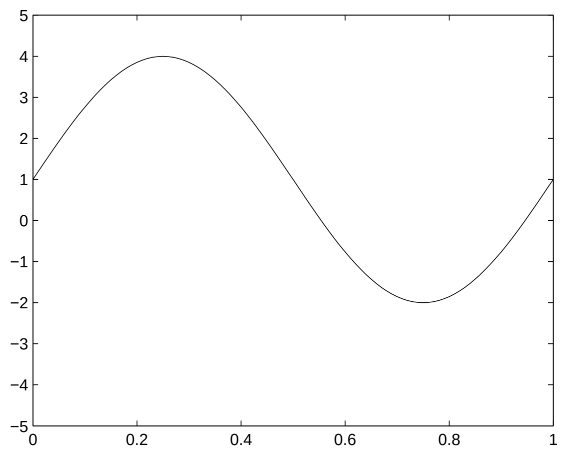
5
4
3
2
1
0
−1
−2
−3
−4
−5
0
0.2
0.4
0.6
0.8
1

Chapter 7

Shallow Water Equations

The shallow water equations may be used for modelling fluid flow in situations where the vertical motion can be considered insiginificant in comparision to the horizontal motion. The equations desribe the flow of a fluid at a single pressure height and are not able to model factors which vary with height. For the use of the equations to be appropriate, the wavelength of the phenonmenon being modelled must be much larger than the depth of the fluid. This means that, in spite of the name, shallow water equations may be used in deep ocean basins if we are modelling tidal motion due to the large tidal wavelength.

The stationary DG method has been applied to many shallow water problems, with Yu and Kyozuka [17] investigating both tidal flows and the dam-break problem. For application of the moving mesh algorithm developed in Chapter 5, we shall look particularly at shallow water equations applied o muia Eow wn siser

7.1.1 The inclusion of boundary speeds

The conservation law problem (7.4, 7.4) must be reworked to include boundary speeds $\dot{x}$.

To include the boundary speeds into the first shallow water equation, we follow the derivation in Chapter 5.

We use Leibniz rule

$$\frac{d}{dt}\int_{x_{j-1/2}}^{x_{j+1/2}} m dx = m\dot{x}|_{x_{j+1/2}} - m\dot{x}|_{x_{j-1/2}} + \int_{x_{j-1/2}}^{x_{j+1/2}} \frac{\partial m}{\partial t} dx$$

to expand

$$\frac{d}{dt}\int_{x_{j-1/2}}^{x_{j+1/2}} vh \, dx.$$

Taking $m = vh$ where $v(x)$ moves with $\frac{dx}{dt}$, we have

$$\frac{d}{dt}\int_{x_{j-}}^{x_{j+1/2}}$$

To include the boundary speeds into the second shallow water equation, we again follow the derivation in Chapter 5, and obtain

$$\frac{d}{dt}\int_{x_{j-1/2}}^{x_{j+1/2}} vQ\,dx = \int_{x_{j-1/2}}^{x_{j+1/2}} v\left(\frac{\partial}{\partial x}(Q\dot{x}) + \frac{\partial Q}{\partial t}\right) dx + \int_{x_{j-1/2}}^{x_{j+1/2}} Q\left(\frac{\partial v}{\partial t} + \dot{x}\frac{\partial v}{\partial x}\right) dx.$$

Again, we take $v(x)$ to move with $\frac{dx}{dt}$ so the last integral on the right-hand side disappears. However, now when we substitute in from the second shallow water equation (7.3), we have an additional term as the right-hand side of (7.3) is non-zero.

$$\frac{d}{dt}\int_{x_{j-1/2}}^{x_{j+1/2}} vQ\,dx = \int_{x_{j-1/2}}^{x_{j+1/2}} v\left(\frac{\partial}{\partial x}(Q\dot{x}) - \frac{\partial}{\partial x}\left(\frac{1}{2}gh^2 + \frac{Q^2}{h}\right) - gh\frac{\partial B}{\partial x}\right) dx.$$

Using integration by parts, this may be rewritten as

$$\frac{d}{dt}\int_{x_{j-1/2}}^{x_{j+1/2}} vQ\,dx = -\left[v\left(\left(\frac{1}{2}gh^2 + \frac{Q^2}{h}\right) - \dot{x}Q\right)\right]$$

$\forall j = 1, \ldots, N$

$$\frac{d}{dt}\int_{x_{j-1/2}}^{x_{j+1/2}} v_h \begin{pmatrix} h_h \\ Q_h \end{pmatrix} dx = -v_h \begin{pmatrix} h_h u_h - \dot{x} h_h \\ \frac{1}{2} g h_h^2 + \frac{Q_h^2}{h_h} - \dot{x} Q_h \end{pmatrix} \Bigg|_{x_{j-1/2}}^{x_{j+1/2}}$$

$$+ \int_{x_{j-1/2}}^{x_{j+1/2}} \begin{pmatrix} h_h u_h - \dot{x} h_h \\ \frac{1}{2} g h_h^2 + \frac{Q_h^2}{h_h} - \dot{x} Q_h \end{pmatrix} \frac{\partial v_h}{\partial x} dx - \int_{x_{j-1/2}}^{x_{j+1/2}} \begin{pmatrix} 0 \\ v_h g h_h \frac{\partial B}{\partial x} \end{pmatrix} dx \tag{7.6}$$

$$\int_{x_{j-1/2}}^{x_{j+1/2}} \begin{pmatrix} h_h(x,0) \\ Q_h(x,0) \end{pmatrix} v_h \, dx = \int_{x_{j-1/2}}^{x_{j+1/2}} \begin{pmatrix} h\ (x) \\ h\ (x) u\ (x) \end{pmatrix} v_h \, dx \tag{7.7}$$

We note that

$$F = \begin{pmatrix} f \\ f_2 \end{pmatrix} = \begin{pmatrix} h_h u_h - \dot{x} h_h \\ \frac{1}{2} g h_h^2 + \frac{Q_h^2}{h_h} - \dot{x} Q_h \end{pmatrix}$$

is undefined at cell boundaries due to this discontinuities in h_h, u_h

7.1.3 Choosing boundary speeds

In the full-DG method from Chapter 5, the boundary speeds are taken as the local shock speeds at each boundary (5.6). However, we now ha

- Solve (7.9, 7.11) to obtain $w_j(0)$, $w_j(0)$, $z_j(0)$, and $z_j(0)$ and hence find $h_h(t = 0)$, $Q_h(t = 0)$;
- For $m = 0, \ldots, M - 1$,
  -

Chapter 8

Numerical Results for Shallow Water Equations

The full-DG moving mesh method with fixed speed adjustements to control cell distribution has been derived for a 1D system of shallow water equations in Chaptershallow. We now apply the method to two simple test problems, firstly considering the dam-break problem, as considered by Yu and Kyozuka [17], and then a tidal bore.

8.1 A Dam-Break

The dam-break problem, with a well-documented solution, has been frequently used as a preliminary test for modelling a system of shallow water equations. The set-up usually starts with the fluid being at rest and partioned into two heights by a dam which is then instantaneously removed at $t = 0$ and the fluid begins to flow.

Yu and Kyozuka [17] consider the conservation law problem

$$\frac{\partial}{\partial t}\begin{pmatrix} h \\ Q \end{pmatrix} + \frac{\partial}{\partial x}\begin{pmatrix} hu \\ \frac{1}{2}gh^2 + \end{pmatrix}$$

taking the initial conditions to be

$$h(x,0) = \begin{cases} 1m & \text{if } x \leq 0.5m \\ 0.5m & \text{if} \end{cases}$$

$\frac{\partial B}{\partial x} = 0$, and h therefore represents the surface height, as well as the height of water above the bed.

The conservation law problem to be solved is given by

$$\frac{\partial}{\partial t}\begin{pmatrix} h \\ Q \end{pmatrix} + \frac{\partial}{\partial x}\begin{pmatrix} hu \\ \frac{1}{2}gh^2 + \frac{Q^2}{h} \end{pmatrix} = 0 \qquad \text{on } [0,1] \times [0,T]$$

taking the initial conditions to be

$$h(x,0) \quad =$$

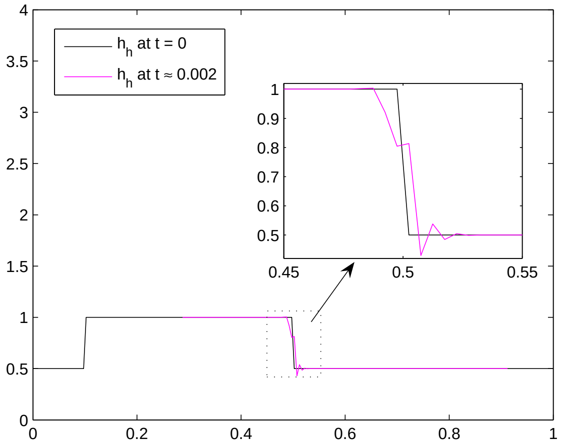

Figure 8.2: The height of the water in the dam-break problem at t = 0.002, found using the full-DG method with stationary boundaries.

We now compare the results for a moving mesh, allowing boundary speeds to be taken as the notional shock speed at each boundary, or fixed at the largest shock speed. To allow some movement, we set the maximum / minimum parameters to be given by

- Initial cell width: $\Delta_j = 0.005$
- Minimum allowed cell width: $\Delta_{j\,min} = 0.005$
- Minimum allowed timestep: $\Delta t_{min} = 0.00001$
- Maximum allowed timestep: $\Delta t_{max} = 0.0001$

Again, we view the solution after 200 steps (t ≈ 0.002) and see in Figure 8.3 that the results are very similar to that of the stationary mesh. If we encourage further movement by reducing the minimum cell width to 0.001, without changing any

l2846936(e)-0.253594 0(l)3-71231(4)-393.517(7)-5183(6)-332.159130.i91steeu distibution algorithm being poorly designed to cope with the multiple shocks that are present.

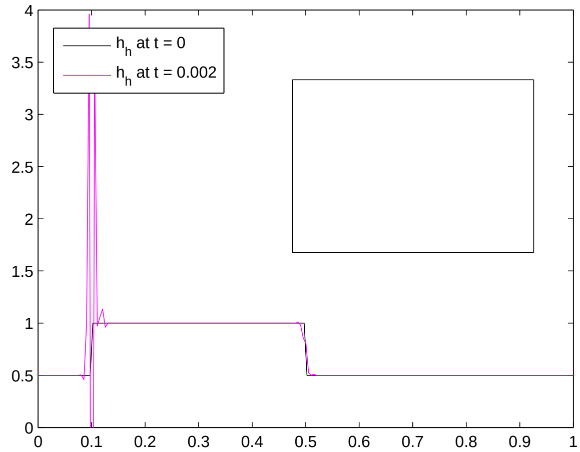

8.2.1 Our problem

The height and speed of a bore is effected by many factors including the height of freshwater in the river, offshore and opposing winds and pressure levels. However, we will assume a very simple model for our bore, and seek to solve the conservation law problem

$$\frac{\partial}{\partial t}\begin{pmatrix} h \\ Q \end{pmatrix} + \frac{\partial}{\partial x}\begin{pmatrix} hu \\ \frac{1}{2}gh^2 + \frac{Q^2}{h} \end{pmatrix} = 0 \qquad \text{on } [0,1] \times [0,T]$$

where

$$\begin{aligned} h(x,0) &= \begin{cases} 2 & \text{if } 0 \le x \le 0.1 \\ (\sin(5 \cdot pi \cdot (x-0.1))).^2 + 2 & \text{if } 0.1 < x < 0.3 \\ 2 & \text{if } 0.3 \le x \le 1 \end{cases} \\ u(x,0) &= 3. \end{aligned}$$

We shall use periodic boundary conditions, as this is how the full-DG method has been developed, although we note that they are unrealistic for a river.

8.2.2 Results

The system was solved for stationary boundaries, setting $\dot{x} = 0$, and the results from an early timestep may be seen in Figure 8.4.

Without any results to compare this to, we cannot be sure that this is giving the correct solution, although the results are plausible, with the inc2351(n)-332.959(e)-0.233s8(h)0.33

Chapter 9

Summary and Further Work

9.1 Summary

This dissertation looked to find a moving mesh method for use with the Discontinuous Galerkin (DG) Finite Element Method , and this has been achieved for a single equation, although only preliminary results were avaliable for the extended algorithm for a 1D system.

We began by considering the stationary Runge-Kutta DG method developed by Cockburn and Shu [11], and commonly used grid adaptation techniques, including velocity-based moving mesh methods. From this, we persued two different routes for obtaining a moving DG method.

Firstly, we considered cell-based moving mesh methods, where the boundary speeds were derived assuming a conservation principle on each cell. Such methods had limited success, possibly due to the use of numerical fluxes, and inconsistencies in the use of the conservation principle which directly links cell widths to the

9.2 Extensions

Due to time constraints, we were unable to fully develop and test a velocity-based moving mesh DG method for a 1D system, and there is the potential for much futher work in this area. The periodicity of the boundary conditions was not realistic for the dam-break and tidal bore test problems, so amending the full-DG method for non-periodic boundary conditions would be a natur could be particularly important for the tidal bore test case, as bores are known to develop in rivers that not only become shallower, but also significantly narrower, creating a funnelling effect on the water.

[16] B.Wells, M.Baines, P.Glaister. Generation of Arbitrary Lagrangian-Eulerian (ALE) Velocities, based on Monitor Functions, for the Solution of Compressible Fluid Equations, International Journal for Numerical Methods in Fluids, Vol.47, pp 1375-1381, (2005).

[17] Z.Yu, Y.Kyozuka. A Discontinous Galerkin Finite Element Shallow Water Model in Simulating Tidal Flows, OCEANS '04. MTS/IEEE TECHNO-OCEAN '04, Vol.3, pp 1526-1531, (2004).

[18] H.Anton, I.Bivens, S.Davis. Calculus, 7th Ed. John Wiley & Sons, Inc, (2002).

[19] K.Eriksson, D.Estep, P.Hansbo, C.Johnson. Computational Differential Equations, Cambridge University Press, (1997).

[20] www.severn-bore.co.uk

[21] www.tidalbore.info